Published in final edited form as:
Stem Cells. 2012 November ; 30(11): 2535–2547. doi:10.1002/stem.1213.

Mitochondrial Superoxide Production Negatively Regulates Neural Progenitor Proliferation and Cerebral Cortical Development

Yan Hou[1], **Xin Ouyang**[1], **Ruiqian Wan**[1], **Heping Cheng**[2], **Mark P. Mattson**[1,3,*], and **Aiwu Cheng**[1,*]

[1] Laboratory of Neurosciences, National Institute on Aging Intramural Research Program, Baltimore, MD 21224

[2] Institute of Molecular Medicine and National Laboratory of Biomembrane and Membrane Biotechnology, Peking University, Beijing 100871, China

[3] Department of Neuroscience, Johns Hopkins University School of Medicine, Baltimore, MD 21205.

Abstract

Although high amounts of reactive oxygen species (ROS) can damage cells, ROS can also play roles as second messengers, regulating diverse cellular processes. Here we report that embryonic mouse cerebral cortical neural progenitor cells (NPCs) exhibit intermittent spontaneous bursts of mitochondrial superoxide (SO) generation (mitochondrial SO flashes) that require transient opening of membrane permeability transition pores (mPTP). This quantal SO production negatively regulates NPC self-renewal. Mitochondrial SO scavengers and mPTP inhibitors reduce SO flash frequency and enhance NPC proliferation, whereas prolonged mPTP opening and SO generation increase SO flash incidence and decrease NPC proliferation. The inhibition of NPC proliferation by mitochondrial SO involves suppression of extracellular signal-regulated kinases. Moreover, mice lacking SOD2 (SOD2−/− mice) exhibit significantly fewer proliferative NPCs and differentiated neurons in the embryonic cerebral cortex at mid-gestation compared with wild type littermates. Cultured SOD2−/− NPCs exhibit a significant increase in SO flash frequency and reduced NPC proliferation. Taken together, our findings suggest that mitochondrial SO flashes negatively regulate NPC self-renewal in the developing cerebral cortex.

Keywords

cpYFP; manganese SOD; extracellular signal-regulated kinases; mitochondrial permeability transition pore; neural progenitor cells; self renewal, proliferation, neurospheres

Introduction

All cells produce reactive oxygen species (ROS), the bulk of which originate when O_2 is converted to superoxide anion radical ($O_2^{\cdot -}$; SO) in mitochondria. SO is dismutated to hydrogen peroxide (H_2O_2) by the activity of mitochondrial superoxide dismutase (SOD2;

*Corresponding authors: (mattsonm@grc.nia.nih.gov) and (chengai@mail.nih.gov), Laboratory of Neurosciences, National Institute on Aging Intramural Research Program, 251 Bayview Blvd, Baltimore, MD 21224. .

Author Contributions: Y.H., M.P.M. and A.C. designed the study; Y.H., X.O. R.W. and A.C. performed the experiments; Y.H. and A.C. analyzed the data; H.C. contributed reagents; Y.H, H.C., M.P.M. and A.C. wrote the manuscript.

Mn-SOD) and cytosolic SOD1; H_2O_2 is then decomposed to water by the activities of glutathione peroxidases and catalase [1, 2]. However, excessive ROS generation and/or impaired detoxification can result in pathological molecular modifications to proteins, nucleic acids and lipids; in addition to SO, two ROS that are particularly damaging are hydroxyl radical (produced from H_2O_2 in a reaction catalyzed by Fe^{2+} and Cu^{+}) and peroxynitrite (produced when SO interacts with nitric oxide). Indeed, oxidative damage to neurons is implicated in a range of neurological conditions including stroke, Alzheimer's disease (AD), Parkinson's disease and Huntington's disease [3, 4]. Although ROS have been mostly studied from the perspective of their roles in disease, it has become clear that ROS also participate in cell signaling events that regulate a range of physiological processes including cell proliferation and differentiation, muscle contraction and synaptic plasticity [5-7].

In contrast to the considerable evidence for the involvement of ROS in a range of physiological and pathological processes in somatic cells, little is known of their roles in stem cells in general, and neural progenitor cells (NPCs) in particular. During brain development, neurons and glial cells are produced from NPCs located in proliferative regions surrounding the lateral ventricles including the ventricular zone (VZ) and subventricular zone (SVZ) [8]. As they differentiate, neurons migrate from the proliferative zone, grow axons and dendrites and form synapses with pre-and post-synaptic neurons to establish their life-long workplace partners [9]. Several signals that regulate the proliferation and differentiation fate of NPCs have been identified including bFGF [10], BDNF [11] and nitric oxide [12]. Signals for self-renewal or differentiation are transduced by intracellular second messengers, kinases and transcription factors [13, 14]. It was previously reported that the proliferation and differentiation of cultured NPCs is affected by the concentration of oxygen in the culture atmosphere, with lower oxygen levels promoting proliferation and higher oxygen levels suppressing proliferation (15-17). A role for ROS in the effects of oxygen tension on NPCs was further suggested by studies showing that ROS levels are low in NPCs and increase upon neuronal differentiation, and that alterations in ROS can affect neuronal differentiation (18). In other studies, different subsets of progenitor cells exhibit different ROS levels, with the most oxidized being more proliferative (19). Thus, accumulated data show that increased ROS suppress stem cell proliferation and promote differentiation in some settings, whereas in other settings cell proliferation is enhanced by ROS. Physiological and pathological conditions that are known to cause ROS production can influence NPC proliferation and differentiation, either positively or negatively, depending upon the intensity and duration of the oxidative stress. For example, mild physiological stresses such as exercise, dietary energy restriction and cognitive challenges increase hippocampal neurogenesis [20]. On the other hand, the proliferation of NPCs is suppressed in diabetes [21] and aging [20]. Therefore, much remains to be learned about the role of ROS in regulating NPC proliferation and differentiation under physiological and pathological conditions.

SOD2 is essential for the survival of aerobic organisms from bacteria to humans (22, 23). The roles of SOD2 in physiological and pathological conditions have recently been reviewed (24, 25). SOD2 may act as either a tumor suppressor or oncogene depending upon differences in redox status of normal, transformed, tumor and metastatic cells (24, 26-28). SOD2 deficient (SOD2−/−) mice exhibit several abnormalities including severe anemia, neurodegeneration, myocardial injuries and prenatal death (29). The function of SOD2 in regulating NPC proliferation and differentiation during development of the nervous system is unknown.

We previously developed a novel mitochondria-targeted fluorescent SO indicator (mt-cpYFP) which was used to demonstrate the existence of spontaneous mitochondrial SO

'flashes' in excitable cells that were dependent upon both electron transport and the transient opening of mitochondrial membrane permeability transition pores (mPTP) [30]. In present study, we found that cerebral cortical NPCs exhibit a distinct pattern of mitochondrial SO flashes, and this mPTP-mediated mitochondrial SO flashes do not appreciably affect global ROS under physiological conditions and exert distinct roles in constraining NPC self-renewal by suppressing MAP kinase activation. Studies of brain development in embryonic SOD2−/− mice revealed a significant reduction of NPC proliferation and neuronal differentiation in the cerebral cortex. Mice lacking SOD2 exhibit elevated SO flash activity and suppression of MAP kinase phosphorylation and NPC proliferation, all of which are rescued by agents that abolish SO flashes. These findings suggest that bursts of mitochondrial SO production negatively regulate NPC proliferation in the developing cerebral cortex.

Materials and Methods

Primary neural progenitor cell neurosphere cultures, treatments and analysis of self-renewal and proliferation

NPCs were prepared from C57 mice or SOD2−/− mice. NPCs isolated from embryonic mouse cerebral cortex were propagated as free-floating aggregates (neurospheres) to promote proliferation of neural stem and progenitor cells for use in experiments as described previously [31, 32]. Briefly, the telencephalon from embryonic day (E) 14.5 mice was dissected in sterile Ca^{2+}- and Mg^{2+}-free Hanks' balanced saline solution (HBSS). The collected cortical tissue was incubated in 0.05% trypsin-EDTA in HBSS for 15 min at 37^0C and then transferred to culture medium for neurosphere (NS) culture medium which consisted of Dulbecco's modified Eagle's medium (DMEM)/F12 (1:1) supplemented with B-27 (InVitrogen, Carlsbad, CA, http://www.invitrogen.com/) and 40 ng/ml basic fibroblast growth factor (bFGF; Becton Dickson, Bedford, MA) and 40 ng/ml epidermal growth factor (EGF; InVitrogen, Carlsbad, CA). These culture conditions were used for all experiments in this study. We cultured dissociated cells from E14.5 telecenphalon at a density of 2×10^5 per ml and total 7 ml (1.4 million cells in total) in 35mm non-coated flasks to grow primary neurospheres. The culture treatments included: 100 μM Tiron, 1 μM TMP, 1 μM MitoTEMPO, 0.1μM cyclosporin A(CsA), 1 μM paraquat (PQ), 1 μM atractyloside (ATR), or 50 μM SS31. All the agents were prepared as 500–1000x stocks in dimethylsulfoxide or distilled water. Mitochondria-targeted tetrapeptide SS31 was a gift from Dr. Heping Cheng of Peking University. Treatments were administered by direct dilution into the culture medium and an equivalent volume of vehicle was added to control cultures. In some experiments, cultures were pretreated with 20 μM PD 98059 (Sigma, St. Louis, MO) for 1h.

Immunocytochemistry and mitochondrial imaging

NPCs or brain sections were processed for immunocytochemistry using the following primary antibodies and dilutions: anti-ß$_3$-tubulin (Tuj1; mouse, 1:250; Sigma, St. Louis, MO), anti-Sox2 (1:200, Chemicon, Temecula, CA), anti-nestin (1:200, Cell Signaling Technology, Danvers, MA), anti Ki67 (1:200, Chemicon, Temecula, CA, http://www.millipore.com/). Secondary antibodies used and their dilutions were: FITC-conjugated donkey anti-mouse (BrdU, Tuj1 and Sox2) or rat (Nestin) or rabbit IgG (Ki67) and rhodamineconjugated donkey anti-mouse IgG(1:500, InVitrogen, Carlsbad, CA).

For immunofluorescence, monolayer NPCs were fixed in a solution of 4% paraformaldehyde in PBS for 20 minutes. The cells or brain sections were permeabilized and preincubated with blocking solution (0.3% Triton X-100, 10% normal goat serum) in PBS for 30 min, and then incubated overnight with a primary antibody diluted in blocking solution at 4°C. Cells or brain sections were washed with PBS and incubated with

appropriate secondary antibodies diluted in blocking solution for 2 h at room temperature. The cells or brain sections were counterstained with propidium iodide (PI) (0.02% PI and 1% RNAse in PBS) for 10 min when needed; they were then washed with PBS and mounted on microscope slides in an anti-fade medium (Vector Laboratories, Burlingame, CA, http://www.vectorlabs.com). For BrdU immunohistochemistry, BrdU was added to the cultures at a final concentration of 10 μM, and at designated time points the cells were fixed in 4% paraformaldehyde in PBS. The immunostaining procedures described above were followed, except that the cells were denatured by incubating in a solution of 2 N HCl for 45 min before the primary antibody was added. To observe mitochondrial morphology, NPCs were transfected with 2 μg pcDNA3.1 plasmid containing mt-dsRED for 24 h. Images were acquired using 25X or 63X objectives on a Zeiss LSM 510 confocal microscope.

Confocal imaging of mitochondrial superoxide production

NPCs were transfected with 2 μg pcDNA3.1 plasmid containing mt-cpYFP coding sequence [30] using FuGENE 6 reagent (Roche Diagonostics, Indianapolis, IN, http://www.rocheusa.com/) according to the instructions of the manufacturer. The imaging was performed 48-72 h after transfection. Confocal imaging used a Zeiss LSM 510 confocal microscope with a 63X, 1.3NA oil immersion objective and a sampling rate of 1.5 s / frame. Dual excitation imaging of mt-cpYFP was achieved by alternating excitation at 405 and 488 nm and emission at 505 nm. Imaging experiments were performed at room temperature (24–26°C). Digital image processing used the Zeiss LSM 510 and sigma plot software (Research Systems), and user-designed programs.

Cell proliferation assays

For monolayer adhesion culture, we cultured dissociated cells from primary neurosphere in PEI-coated dishes at the density of 100×10^3 per cm^2 culture surface area. After NPC cultures were exposed to experimental treatments for designated time periods, bromodeoxyuridine (BrdU) was added to the cultures at a final concentration of 10 μM, and 2 h later the cells were fixed in 4% paraformaldehyde in PBS, processed for immunocytochemistry, and counterstained with PI to label the nucleus of all cells. Images were acquired in five randomly chosen microscope fields using a 25X objective and dual channels for BrdU immunostaining (488 nm excitation and 510 nm emission) and propidium iodide (543 nm excitation and 590 nm emission). The BrdU- and propidium iodide-positive cells were counted simultaneously in each image, and the proliferation index was calculated as the number of BrdU-positive cells divided by the total number of the cells (propidium iodide-positive). A minimum of 3 cultures for each condition were used in each experiment. For neurosphere formation assay, we collected neurospheres on culture day 3 and dissociated them using a NeuroCult cell dissociation kit (StemCell Technologies, Vancouver, Canada, http://www.stemcell.com/) to culture in 96-well non-coated plate with 1000 cells/200 μl culture medium per well to analyze the neurosphere formation from 1000 cells. The number of secondary NS formed from the stem cells was used as a measure of NPC self-renewal. The size (diameter) of the secondary NS was used as a measure of cell proliferation (33, 34). Analyses were performed at 5-7 days in culture; images of NS in 8 wells per experimental condition were acquired and were then analyzed using Adobe Photoshop or NIH Image J software to quantify both the number of NS and the diameter of individual NS. All data presented are the results of 3–4 separate experiments.

Immunoblot analysis

Cultured cells were solubilized in sodium dodecyl sulfate–polyacrylamide gel electrophoresis sample buffer, and the protein concentration in each sample was determined using a Bio-Rad protein assay kit (Bio-Rad, Hercules, CA, http://www.bio-rad.com/) with bovine serum albumin as the standard. Proteins (30 μg of protein per lane) were then

resolved in a 7.5– 10% sodium dodecyl sulfate–polyacrylamide gel and electrophoretically transferred to a nitrocellulose membrane. Membranes were blocked with 4% non-fat milk in TBST (Tris–HCl based buffer with 0.2% Tween 20, pH 7.5), and then incubated in the presence of primary antibody overnight at 4^0C. Cells were then incubated for 1 h in the presence of a 1:5000 dilution of secondary antibody conjugated to horseradish peroxidase (Jackson Immunoresearch Laboratory, West Grove, PA, http://www.jacksonimmuno.com/). Reaction product was visualized using an Enhanced Chemiluminescence Western blot detection kit (Amersham Bioscience, Piscataway, NJ, http://www.biochipnet.com/). The blots were probed with anti-phosphorylated extracellular signal-regulated kinase (ERK) 1/2, phosphorylated p38 and phosphorylated JNK and total ERK1/2 (Cell Signaling Biotechnology, Danvers, MA) and anti-actin (mouse, 1:5000; Sigma, St. Louis, MO).

Cellular ROS measurement

NS were isolated and aliquoted in wells in a 96-well plate (1×10^6 cells per well). To measure intracellular accumulation of ROS, the peroxide sensitive fluorescent probe 5-(and-6)-carboxy-2′7′-dichlorodihydrofluorescein diacetate (DCF; Invitrogen/Molecular Probes, Eugene, OR, http;//www.invitrogen.com/) was used. In brief, DCF was added to cells at a final concentration of 20 μM. The cultures were incubated at 37°C for 30 min. After washing with pre-warmed NPC culture medium, the fluorescence intensity was measured using a plate reader (488 nm excitation and 510 nm emission).

Mitochondrial superoxide dismutase (SOD2) deficient mice: genotyping, BrdU administration and histochemistry

SOD2−/− mice (the *Sod2*^{tm1Leb} targeted mutation) were purchased from Jackson Laboratories (stock no: 002973), which was originally made by R. Lebovitz (29). A 1.5 Kb HindIII fragment containing exons 1 and 2 of the *Sod2* gene, as well as approximately 500bp immediately 5′ of exon 1, was replaced with a human hypoxanthine phosphoribosyltransferase minigene driven by the phosphoglycerate kinase promoter. The transcription and translation start sites, the mitochondrial targeting sequence, and one of the three histidines that bind directly to the manganese cofactor, were eliminated. For genotyping, two complementary PCRs were performed on genomic DNA from mouse tail or tissues. The first reaction used primers for detecting a SOD2 exon 1 sequence (5′ACGTTGCCTTCCCAGGAT 3′ and 5′GTTTACACGACCGCTGCTCT3′) and the second reaction used primers for detecting a mutated sequence (5′TGT TCT CCT CTT CCT CAT CTC C3′ and 5′ACC CTT TCC AAA TCC TCA GC3′). The first reaction generates a 193bp product for the WT allele and the second reaction generates a 240bp product for the mutant allele. For BrdU administration, timed pregnant female mice received bromodeoxyuridine (BrdU) by intraperitoneal injection (50 mg/kg) 1 h before euthanasia by cervical dislocation. The embryos were removed and the tail from each embryo was collected for genotyping. The head of each embryo was immediately fixed in 4% paraformaldehyde. Two days later the fixed brains were transferred to a solution of 30% sucrose in PBS for cryopreservation. Cryostat sections of the brains were cut in the coronal plane at a thickness of 15 μm and collected on Superfrost Plus slides (VWR, West Chester, PA). Brain sections were processed for immunohistochemistry.

Data analysis

All data are presented as mean ± SD. Comparisons between control and treatment groups were performed by using Student′s unpaired *t* test or ANOVA when appropriate. $P < 0.05$ was considered to be statistically significant.

Results

Neural Progenitor Cells Exhibit Spontaneous Bursts of Mitochondrial Superoxide Production

NPC cultures were established from embryonic day 14.5 mouse cerebral neuroepithelium and propagated as free-floating neurospheres to promote proliferation of NPC prior to use in experiments as described previously [31, 32]. When dissociated neurospheres were plated at a high density in polyethyleneimine-coated dishes and maintained for 3 days in presence of bFGF and EGF, approximately 98% of the cells were proliferating NPCs as demonstrated by their expression of the NPC markers Sox2 and nestin, and by incorporation of BrdU into their DNA (Fig. 1A). NPCs displayed bipolar and round morphologies. Mitochondrial subcellular localization and morphology was evaluated in cultured NPCs transfected with mt-DsRed plasmid. Unlike mitochondria in cultured embryonic hippocampal neurons which exhibit a distinct rod-like morphology (Fig. S1), mitochondria in NPCs displayed a reticulum-like structure concentrated around the nucleus (Fig. 1A).

Cultured NPCs stably expressing mitochondrial SO sensor mt-cpYFP [30], exhibited a weak basal fluorescence signal with the same mitochondrial localization observed in mt-DsRed-labeled cells (Fig. 1B, 1D). When imaged during a 5 minute period, approximately 10% of the NPCs exhibited one or more robust, transient increase in mt-cpYFP fluorescence kinetically similar to the “SO flashes” previously observed in cardiac myocytes and embryonic neurons [30]. The SO flashes in the NPCs typically peaked within 2-4 seconds then decreased to baseline levels within 5-7 seconds (Fig 1B-1E; Supplemental movie 1 and 2). These SO flash events were observed at 488 nm excitation and exhibited all-or-none properties (Fig. 1B-1E). In contrast, when excited at 405 nm the emitted fluorescence signal was unchanged (data not shown). The mitochondrial SO flashes appeared to occur randomly among the NPCs. However, mitochondria adjacent to each other throughout the cell (Fig. 1B) or in a perinuclear location (Fig. 1D) exhibited SO flashes that occurred in a synchronized manner, suggesting the presence of a mitochondrial reticulum or molecular communication among closely apposed individual mitochondria. These communal mitochondrial SO flashes in the NPCs contrast with the autonomous single mitochondrial flashes observed in cardiomyocytes or neurons in a previous study [30].

Regardless of subcellular localization (perinuclear or in cell processes), mitochondrial SO flashes were indistinguishable in their amplitude and kinetics (Fig. 1F-1I). A typical flash arises abruptly, peaks in 2.9 ± 0.98 s and dissipates with a half-time of 4.08 ± 1.6 s (mean + SD of 47 flashes). The average fractional peak increase of mt-cpYFP fluorescence ($\Delta F/F0$) during a flash was 0.29 ± 0.11 (mean + SD of 47 flashes). Flash generation can be manipulated by pharmacological agents that affect mPTP opening and SO scavenging in cardiac myocytes [30]. We found that the incidence of mitochondrial SO flashes was reduced by approximately 80% in NPCs treated with the mitochondrial SO scavengers mitoTEMPO (1 μM) and tetrapeptide SS31 (D-Arg-Dmt-Lys-Phe-NH2; 50 μM), the SOD2 mimetic MnTMPyp (TMP, 1μM), the SO scavenger Tiron (100 μM), or the mitochondrial mPTP inhibitor Cyclosporin A (CsA, 0.1 μM) (Fig. 2A). Application of the mitochondrial SO generator paraquat PQ (1 μM), or the mPTP opener ATR (1 μM) increased flash frequency by 89% and 63%, respectively (Fig. 2A). Collectively, these findings suggest that NPCs exhibit SO flashes that are generated by a mechanism involving a functional coupling of transient mPTP opening with a rapid burst of SO generation.

To determine whether the agents that reduce mitochondrial SO flash activity also reduce global ROS levels, we measured DCF fluorescence intensity in NPCs exposed to the same agents. Interestingly, the mitochondrial SO flashes did not contribute appreciably to global ROS levels because manipulations that reduced or enhanced mitochondrial SO flash

incidence did not affect basal global ROS levels (DCF fluorescence intensity, Fig. 2B). These findings suggest that mPTP-mediated SO flashes are quantal mitochondrial events that do not affect global ROS homeostasis appreciably under physiological conditions.

Superoxide Flashes Negatively Regulate the Proliferation of NPCs

We next explored the function of SO flashes in NPCs. Because ROS can act as signaling molecules that regulate cell proliferation, we determined whether spontaneous SO flashes influence the proliferation of NPCs. First, we quantified the numbers of neurospheres formed from equal numbers of dissociated NPCs during a 6 day culture period; the cultures were treated at the time of plating with vehicle (control) or pharmacological agents at concentrations that blocked SO flash biogenesis. Neurosphere numbers and diameters were both dramatically enhanced in cultures treated with MitoTEMPO and SS31compared with control cultures. Neurosphere numbers, but not diameters were significantly greater in cultures treated with TMP, Tiron and CsA (Fig. 3A, 3C, 3D). We also measured BrdU incorporation in cultures of dissociated NPCs growing on an adherent substrate. Compared to control cultures, significantly more NPCs incorporated BrdU in cultures treated with agents that reduce SO flash incidence (Fig. 3B, 3E). In contrast, neurosphere numbers and diameters were significantly decreased in cultures treated with PQ and ATR, agents that enhanced mitochondrial SO flash incidence (Fig. 3F, 3G). Significantly fewer NPCs incorporated BrdU in cultures treated with PQ or ATR compared to control cultures (Fig. 3H). As we demonstrated previously (Fig.2B), the reagents that either enhance or reduce SO flash incidence do not affect global ROS. Therefore, these findings suggest that the burst production of mitochondrial SO (SO flash) negatively regulates NPC proliferation, by a mechanism not involving changes in global ROS. We further examined SO flash activity in NPCs cultured in an atmosphere with a reduced concentration of O_2 (5%). We found that SO flash incidence was reduced by 60% in NPCs cultured with 5% O_2 compared to the usual higher O_2 concentration of 21% (Fig. S2A). NPCs cultured with 5% O_2 showed a significant increase in proliferation compared to those cultured in a 21% O_2 atmosphere as indicated by a 20% increase in BrdU incorporation and a 38% increase in neurosphere number (Fig. S2B, S2C). These results further support our conclusion that mitochondrial SO production is negatively associated with NPC proliferation.

Superoxide Flashes Suppress ERK Activity

Mitogen-activated protein (MAP) kinases function in a variety of signal transduction pathways and play important roles in regulating cell growth, differentiation, and survival. Members of the MAP kinase family include the extracellular signal-regulated kinases (ERK-1/p44 MAP kinase and ERK-2/p42 MAP kinase), Jun N-terminal kinase (JNK), and p38 MAP kinase [35]. ERKs are typically activated by growth factor stimulation and promote cell proliferation, differentiation and/or survival of stem cells. In contrast, JNK and p38 MAP kinases are strongly activated by a variety of cellular stresses and are involved in apoptosis and inflammatory responses [36]. We therefore determined whether one or more of the MAP kinases were activated or inhibited by SO flash activity in NPC. We found that exposure of NPCs to agents that reduce SO flashes for 24 hours resulted in significant elevations in the level of phosphorylated ERK1 and ERK2 (p-ERKs), without a change in the overall level of ERKs 1 and 2 (Fig. 4A, 4B). In contrast, treatment of NPCs with these agents for 24 hours did not affect levels of phosphorylated JNK or p38 (Fig. 4A). We next employed PD98059, an inhibitor of the ERK-activating kinase MEK-1, to determine whether inhibition of ERK activation was sufficient to account for the inhibition of NPC proliferation by SO flash. Treatment of NPCs with PD98059 alone significantly reduced the proliferation of NPCs, and completely blocked the abilities of MitoTEMPO, SS31, TMP, Tiron and CsA to enhance NPC proliferation (Fig. 4C). Collectively, these results suggest

that quantal mitochondrial SO flashes serve a signaling role by reducing ERK activity which, in turn, reduces NPC proliferation.

Genetic deletion of SOD2 results in reduced NPC proliferation and neuronal differentiation in the embryonic cerebral cortex

To elucidate the roles of mitochondrial SO in the regulation of NPC fate in vivo, we employed a line of SOD2-deficient (SOD2−/−) mice that die within the first few weeks of birth at which time they exhibit severe anemia, weakness, motor dysfunction and degeneration of neurons and cardiac myocytes (29). At a mid-gestational stage of embryonic development (E14.5), the cerebral cortex of SOD−/− mice appeared smaller than wild type control embryos. To determine the extent to which the cells in each layer in a radial unit of the developing cortex differed in SOD−/− and wild type embryos, we examined the frontal cortex in coronal sections immunostained with Tuj1 (a marker of differentiated neurons) and Ki67 (a marker of proliferative cells which are exclusively NPCs at this specific developmental stage) (37, 38). In both wild type and SOD2−/− embryos, Ki67+ and Tuj1+ cells demark a clear germinal zone (proliferative zone) and zones of differentiated neurons (intermediate and cortical plate zones), respectively (Fig. 5A). The thickness of the developing cerebral cortex was reduced in SOD2−/− mice. The thickness of proliferative zone (NPC zone) was significantly reduced by 15%, and the overall thickness of the differentiated layer of neurons (IZ and CP) was reduced by 22%, in the SOD2−/− mice compared to wild type littermate embryos (Fig. 5A-C). The thinning of the germinal zone thinning was due to decreased NPC proliferation rather than increased cell death because TUNEL-positive (apoptotic) cells were rare in brain sections from both wild type and SOD2−/− mice (data not shown). The significant reduction of differentiated neurons in the developing cortex of SOD2-deficient mice may therefore result from reduced NPC proliferation, a possibility consistent with our evidence that mitochondrial SO negatively regulates the proliferation of cultured NPCs.

To determine whether the proliferation of NPCs is altered in SOD2−/− mice, we pulse-labeled developing embryos with the DNA precursor BrdU by administering BrdU to pregnant dams carrying E14.5 embryos. One hour after the BrdU pulse the embryos were removed and brain sections were prepared and immunostained with a BrdU antibody (Fig. 5D). During early brain development, NPCs in the germinal zone exhibit interkinetic nuclear migration with S phase at the pial side and mitosis at the ventricular surface (surface dividing) (39). We found that interkinetic nuclear migration occurred in both SOD2−/− and wild type mice. BrdU+ cells were present in the zone at the pial side, corresponding to S phase cells, whereas few BrdU+ cells were present on the ventricular surface which is expected with a 1 hour BrdU pulse-label. BrdU+ cells were quantified in a 200 μm wide slab oriented perpendicular to the developing cortical wall at the level of frontal cortex (Fig. 5A, D). There are approximately 34.5% fewer BrdU+ cells at E14.5 in the proliferative zone of SOD2−/− mice compared to wild type mice (Fig. 5E). These data indicate that the proliferation of NPCs in the germinal zone is significantly reduced, resulting in cortical dysgenesis.

Mitochondrial SO production underlies the reduced proliferation of NPC in SOD2-deficient mice

When neurosphere cultures derived from the E14.5 telecephalon of SOD2−/− mice were compared with those from WT mice, we found that NPC self-renewal ability *in vitro* is also impaired in embryonic NPCs, which is consistent with above *in vivo* data. NPCs from SOD2−/− mice formed significantly fewer and smaller neurospheres (Fig. 6A, B), and significantly less NPCs incorporated BrdU in cultures from SOD2−/− mice compared to NPCs from wild type mice (Fig. 6A, B).

To test whether mitochondrial SO production is dysregulated in SOD2−/− mice, we imaged SO flash occurrence by stably expressing the mitochondrial SO sensor mt-cpYFP in cultured NPCs. NPCs from SOD2−/− mice exhibited a flash frequency 81% greater than that from wild type littermates (Fig. 6C), demonstrating that SOD2 deficiency increases spontaneous bursts of SO production. In parallel NPC cultures, we measured global ROS levels by quantifying the DCF fluorescence intensity. The basal global ROS level in wild type NPCs was low, and SOD2-deficient NPCs exhibited a significant elevation of basal ROS (Fig. 6D).

To determine whether increased mitochondrial SO production is responsible for the reduced proliferation of NPCs lacking SOD2, we used pharmacological agents to suppress SO flashes (Fig. 2A), and then measured SO flashes and cell proliferation. TMP, MitoTEMPO and CsA each suppressed the SO flashes in SOD2−/− NPCs (Fig. 7A). When simultaneously measuring global ROS by quantifying DCF fluorescence intensity, we found that exposure of SOD2−/− NPCs to CsA that abolished flash incidence did not result in a significant reduction global ROS levels, whereas treatment with TMP and MitoTempol resulted in significant reductions in global ROS levels in SOD2−/− NPCs (Fig. 7B). Consistent with previous data (Fig. 3A), SOD2−/− NPCs, in which SO flash activity was significantly elevated, exhibited dramatic reductions in the levels of p-ERK1 and p-ERK2 (Fig.7C). Treatment of SOD2−/− NPCs with mitoTEMPO, TMP and CsA prevented the reduction on phosphorylation of ERK1 and ERK2 (Fig. 7C). Finally, we found that the proliferation of dissociated NPCs lacking SOD2 was suppressed compared to wild type NPCs, and that this reduction of NPC proliferation was rescued by treatment with agents that reduce mitochondrial SO levels (Fig. 7D). Collectively, these findings suggest that elevated mitochondrial SO flash activity negatively regulates NPC proliferation by a mechanism involving suppression of ERKs.

Discussion

By measuring and manipulating mitochondrial SO production, we provide evidence for several previously unknown roles for bursts of mitochondrial SO production in NPC biology and development of the cerebral cortex: 1) SO flashes negatively regulate NPC proliferation under physiological conditions; 2) The generation of SO flashes is coupled to inhibition of ERKs; 3) NPCs lacking SOD2 exhibit increased SO bursts and reduced proliferation in cell culture and in vivo; and 4) The proliferation of NPCs and the production of neurons are reduced in the embryonic cerebral cortex of SOD2-deficient mice. In a physiological setting, cultured cortical NPCs display spontaneous SO flash activity, which occurs in clusters of mitochondria in perinuclear regions or processes of bipolar NPCs. The amplitude of individual SO flashes is very similar among NPCs suggesting that the transient bursts of SO arise by a tightly controlled mechanism. We found that SO flashes were abolished in NPCs incubated in the presence of mitochondrial SO scavenger and inhibitor of the mitochondrial mPTP, indicating that the SO flashes required mitochondrial SO production and transient opening of the mPTP. Further analyses provided evidence that SO negatively regulates NPC proliferation by inhibiting the activation of ERKs. In vivo, there are significant reductions of NPCs in the germinal zone of the cerebral cortex in mid-gestational SOD2−/− mice. Cultured SOD2−/− NPCs exhibited a significant elevation of mitochondrial SO flash activity which mediated the suppression of reduced cell proliferation.

Time-lapse confocal imaging of mitochondrial SO levels in NPCs using a novel mitochondria-targeted cp-YFP probe revealed that the NPCs exhibit spontaneous bursts of mitochondrial SO production with features similar to the SO “flashes” recently described in excitable cardiac myocytes and neurons [30]. The amplitude and kinetics of typical mitochondrial SO flashes in NPCs are similar to those in myocytes or neurons. However, in

cardiac myocytes and neurons, SO flashes occur within single mitochondria with no evidence of SO flashes occurring in one mitochondrion affecting the probability of a SO flash occurring in an adjacent mitochondrion [30]. In contrast, SO flashes in NPCs are often synchronized among clusters of mitochondria, particularly those located in a perinuclear region. The mechanism by which SO flashes occur synchronously among mitochondria in NPC is unknown, but may be a result of a reticular network of mitochondria or possibly an inter-mitochondrial signaling system. We also find that mitochondrial SO flashes occurring in NPCs are blocked by SO scavengers (MitoTEMPO, SS31, TMP and Tiron) and by the mPTP inhibitor CsA. SO flash frequency is enhanced by the mitochondrial SO generator PQ, by the mPTP opener ATR, and by genetic deletion of MnSOD. These findings suggest there is a functional coupling between transient mPTP opening and bursts of mitochondrial SO generation, which underlies the mechanism of mitochondrial SO flash generation in NPCs. Our evaluation of the relationship between global ROS and mitochondrial ROS in the form of SO flashes revealed that agents that selectively affect mitochondrial SO production and SO flash frequency do not have a discernible effect on global ROS levels as measured using the probe DCF. This could be accounted for by the spatial confinement, temporal brevity, and low frequency of SO flashes in NPCs under physiological conditions. All of the pharmacological agents that blocked the mitochondrial SO flashes significantly increased secondary neurosphere number by 26-34%, which suggests that blocking SO flash activity promotes NPC self-renewal. Treatment of neurospheres with MitoTempol and SS31 resulted in a significant (15-17%) increase of neurosphere size, whereas TMP, Tiron and CsA treatment did not significantly affect neurosphere size. Collectively, these findings suggest pivotal roles for transient opening of mitochondrial PTPs and SO flashes in NPC self-renewal, and a less prominent role for mitochondrial SO flashes in the proliferation of NPC. The NPC have the ability to undergo either a symmetrical cell division, resulting in two new daughter NPCs, or an asymmetric cell division resulting in one self-renewing daughter cell and one neuron. NPC undergoing symmetrical divisions have a relatively high mitotic rate and can generate more cells in a given time period compared to NPC that divide asymmetrically. The differences in the effects of these pharmacological agents may be due to their differential regulation of genes that influence the different mode of cell division. These findings demonstrate that mitochondrial SO flashes negatively regulate the self-renewal of NPCs. In support of this conclusion, we also found the self-renewal and proliferation rate of NPCs were significantly decreased when SO flashes were enhanced by treatment of the cells with SO generator PQ and mPTP opener ATR.

We found that suppression of SO flash activity promotes activation of ERKs 1 and 2 kinases previously shown to enhance the proliferation of embryonic stem cells [40] and NPCs [41, 42]. Conversely, high levels of mitochondrial SO flash activity in SOD2−/− NPCs suppressed NPC proliferation by inhibition of activity of ERKs 1 and 2. Since our data demonstrate that SO flashes make only a negligible contribution to the global ROS level, they provide evidence for a previously unknown role for mPTP-mediated bursts of mitochondrial SO in regulating NPC self-renewal. Although the central role of ERKs in responses of cells to growth factors has been demonstrated, mechanisms controlling dynamic features of ERK phosphorylation are incompletely understood. It has been reported that the activation of ERK signaling can undergo oscillations with a periodicity of 1 – 2 hours, but the factors controlling such oscillations and their physiological roles are unknown [43]. We found that SO flashes inhibit ERK phosphorylation, and that multiple pharmacological agents that block SO flashes enhance NPC proliferation. It is possible that bursts of mitochondrial SO production play a role in the oscillatory nature of ERK activity. Moveover, SOD2−/− NPCs exhibited a significant increase in flash incidence and displayed reductions of ERK phosphorylation and NPC proliferation. Therefore, our findings further suggest that SO flashesfunction in a novel signaling pathway that regulates NPC proliferation by modulating the phosphorylation of ERKs SODs, including cytosolic and

extracellular SODs (SOD1 and SOD3) and SOD2, are major antioxidant defense enzymes. Inactivation of SOD1 and SOD3 in mice results in mild nonlethal phenotypes (44, 45). In contrast, inactivation of SOD2 results in neonatal lethality characterized by neurodegeneration, anemia, and dilated cardiomyopathy, Oxidative DNA damage, impaired electron transport chain function, and abnormalities in tricarboxylic acid cycle enzymes (29, 46, 47). This emphasizes the importance of mitochondrial SOD and mitochondrial SO. However, the function of SOD2 in early brain development, particularly in NPC self-renewal capacity, was previously unknown. In the present study we show that SOD2 deficiency results in significant reductions in numbers of NPCs and differentiated (Tuj1-positive) neurons in mid-gestational embryonic frontal cortex, which results in a dramatic thinning of the cerebral wall. Our BrdU pulse-labeling studies revealed that SOD2 deficiency results in significantly fewer proliferative NPCs cells in neurosphere cloning assays and in the developing embryonic cerebral cortex in vivo. SOD2 deficiency did not result in any discernible increase in apoptotic cells in the developing cerebral cortex, consistent with a reduction in NPC proliferation being the major consequence of elevated mitochondrial SO production that retards expansion of the embryonic cerebral cortex. NPC lacking SOD2 exhibited significant increase SO flash incidence. The global ROS in WT NPC cells is, in general, very low. SOD2−/− NPCs did exhibit a small (~1.5 fold of WT NPC) and significant elevation of DCF fluorescence intensity. Intriguingly, treatment of TMP, MitoTempol and CSA all abolished SO flashes and rescued the proliferation suppression in SOD2−/− NPC. However, unlike TMP and MitoTempol, treatment of NPCs with CsA, which abolished the SO flashes in SOD2−/− NPCs, did not affect global ROS. Therefore, our analysis of embryonic SOD2−/− NPCs suggests a prominent role for mitochondrial SO flashes in the negative regulation of NPCs in vivo. Our findings also reveal transient mPTP opening-triggered SO flashes which are distinct from constitutive ROS production. SO flash events provide a novel frequency-dependent mechanism to activate a local ROS signaling pathway, which can transiently suppress phosphorylation of ERK in the cells where the global ROS concentration remains low.

In a review article on the roles of ROS in the regulation of stem cell fate, Noble et al. (2005) (48) concluded that “It is not yet clear how cells can interpret putatively identical signals in such opposite manners, but it does already seem clear that resolving this paradox will provide insights of considerable relevance to the understanding of normal development, tissue repair, and tumorigenesis.” Our findings help to resolve this seeming paradox by demonstrating that specific, focal and temporally-constrained bursts of mitochondrial SO negatively regulate NPC proliferation independently of the kinds of global changes of ROS studied previously. By integrating our findings with those of others (29, 49, 50, 51), we propose that dynamic mitochondrial ROS generation in the form of mPTP-dependent SO flashes serves as a signaling mechanism that controls the fate of NPCs. Our findings suggest that there is considerable complexity and specificity regarding the subcellular localization and temporal coding of ROS generation, and the molecular targets/mechanisms of action of ROS in regulating NPC fate.

Supplementary Material

Refer to Web version on PubMed Central for supplementary material.

Acknowledgments

This work was supported by the Intramural Research Program of the National Institute on Aging, and by the National Natural Science Foundation and National Basic Research Program of China (2011CB809100).

References

1. Day BJ. Catalase and glutathione peroxidase mimics. Biochem Pharmacol. 2009; 77:285–296. [PubMed: 18948086]
2. Mattson MP, Gleichmann M, Cheng A. Mitochondria in neuroplasticity and neurological disorders. Neuron. 2008; 60:748–766. [PubMed: 19081372]
3. Halestrap AP, Kerr PM, Javadov S, et al. Elucidating the molecular mechanism of the permeability transition pore and its role in reperfusion injury of the heart. Biochim Biophys Acta. 1998; 1366:79–94. [PubMed: 9714750]
4. Lin MT, Beal MF. Mitochondrial dysfunction and oxidative stress in neurodegenerative diseases. Nature. 2006; 443:787–795. [PubMed: 17051205]
5. Goldhaber JI, Qayyum MS. Oxygen free radicals and excitation-contraction coupling. Antioxid Redox Signal. 2000; 2:55–64. [PubMed: 11232601]
6. Maulik N, Das DK. Redox signaling in vascular angiogenesis. Free Radic Biol Med. 2002; 33:1047–1060. [PubMed: 12374616]
7. Kishida KT, Klann E. Sources and targets of reactive oxygen species in synaptic plasticity and memory. Antioxid Redox Signal. 2007; 9:233–244. [PubMed: 17115936]
8. Luskin MB. Neuroblasts of the postnatal mammalian forebrain: their phenotype and fate. J Neurobiol. 1998; 36:221–233. [PubMed: 9712306]
9. Mattson MP, Bruce-Keller AJ. Compartmentalization of signaling in neurons: evolution and deployment. J Neurosci Res. 1999; 58:2–9. [PubMed: 10491567]
10. Carpenter MK, Cui X, Hu ZY, et al. In vitro expansion of a multipotent population of human neural progenitor cells. Exp Neurol. 1999; 158:265–278. [PubMed: 10415135]
11. Benraiss A, Chmielnicki E, Lerner K, et al. Adenoviral brain-derived neurotrophic factor induces both neostriatal and olfactory neuronal recruitment from endogenous progenitor cells in the adult forebrain. J Neurosci. 2001; 21:6718–6731. [PubMed: 11517261]
12. Cheng A, Wang S, Cai J, et al. Nitric oxide acts in a positive feedback loop with BDNF to regulate neural progenitor cell proliferation and differentiation in the mammalian brain. Dev Biol. 2003; 258:319–333. [PubMed: 12798291]
13. Dworkin S, Mantamadiotis T. Targeting CREB signalling in neurogenesis. Expert Opin Ther Targets. 2010; 14:869–879. [PubMed: 20569094]
14. Rafalski VA, Brunet A. Energy metabolism in adult neural stem cell fate. Prog. Neurobiol. 2011; 93:182–203. [PubMed: 21056618]
15. Smith J, Ladi E, Mayer-Proschel M, et al. Redox state is a central modulator of the balance between self-renewal and differentiation in a dividing glial precursor cell. Proc Natl Acad Sci U S A. 2000; 97:10032–10037. [PubMed: 10944195]
16. Morrison SJ, Csete M, Groves AK, et al. Culture in reduced levels of oxygen promotes clonogenic sympathoadrenal differentiation by isolated neural crest stem cells. J Neurosci. 2000; 20:7370–7376. [PubMed: 11007895]
17. Studer L, Csete M, Lee SH, et al. Enhanced proliferation, survival, and dopaminergic differentiation of CNS precursors in lowered oxygen. J Neurosci. 2000; 20:7377–7383. [PubMed: 11007896]
18. Tsatmali M, Walcott EC, Crossin KL. Newborn neurons acquire high levels of reactive oxygen species and increased mitochondrial proteins upon differentiation from progenitors. Brain Res. 2005; 1040:137–150. [PubMed: 15804435]
19. Le Belle JE, Orozco NM, Paucar AA, et al. Proliferative neural stem cells have high endogenous ROS levels that regulate self-renewal and neurogenesis in a PI3K/Akt-dependant manner. Cell Stem Cell. 2011; 8:59–71. [PubMed: 21211782]
20. Lazarov O, Mattson MP, Peterson DA, et al. When neurogenesis encounters aging and disease. Trends Neurosci. 2010; 33:569–579. [PubMed: 20961627]
21. Stranahan AM, et al. Diabetes impairs hippocampal function through glucocorticoid-mediated effects on new and mature neurons. Nat Neurosci. 2008; 11:309–317. [PubMed: 18278039]
22. Gregory EM, Fridovich I. Oxygen toxicity and the superoxide dismutase. J Bacteriol. 1973; 114(3):1193–1197. [PubMed: 4197269]

23. Saltzman HA, Fridovich I. Editorial: Oxygen toxicity. Introduction to a protective enzyme: superoxide dismutase. Circulation. 1973; 48(5):921–923. [PubMed: 4584616]
24. Miriyala S, Holley AK, St Clair DK. Mitochondrial superoxide dismutase--signals of distinction. Anticancer Agents Med Chem. 2011; 11(2):181–190. [PubMed: 21355846]
25. Holley AK, Dhar SK, Xu Y, et al. Manganese superoxide dismutase: beyond life and death. Amino Acids. 2012; 42(1):139–158. [PubMed: 20454814]
26. Buettner GR. Superoxide dismutase in redox biology: the roles of superoxide and hydrogen peroxide. Anticancer Agents Med Chem. 2011; 11(4):341–346. [PubMed: 21453242]
27. Fridovich I. Superoxide dismutases: anti-versus pro-oxidants? Anticancer Agents Med Chem. 2011; 11(2):175–7. [PubMed: 21182471]
28. MacMillan-Crow LA, Crow JP. Does more MnSOD mean more hydrogen peroxide? Anticancer Agents Med Chem. 2011; 11(2):178–180. [PubMed: 21291402]
29. Lebovitz RM, Zhang H, Vogel H, et al. Neurodegeneration, myocardial injury, and perinatal death in mitochondrial superoxide dismutase-deficient mice. Proc Natl Acad Sci U S A. 1996; 93(18): 9782–7. [PubMed: 8790408]
30. Wang W, Fang H, Groom L, et al. Superoxide flashes in single mitochondria. Cell. 2008; 134:279–290. [PubMed: 18662543]
31. Cheng A, Coksaygan T, Tang H, et al. Truncated tyrosine kinase B brain-derived neurotrophic factor receptor directs cortical neural stem cells to a glial cell fate by a novel signaling mechanism. J Neurochem. 2007; 100:1515–1530. [PubMed: 17286628]
32. Lathia JD, Okun E, Tang SC, et al. Toll-like receptor 3 is a negative regulator of embryonic neural progenitor cell proliferation. J Neurosci. 2008; 28:13978–13984. [PubMed: 19091986]
33. Torroglosa A, Murillo-Carretero M, Romero-Grimaldi C, et al. Nitric oxide decreases subventricular zone stem cell proliferation by inhibition of epidermal growth factor receptor and phosphoinositide-3-kinase/Akt pathway. Stem Cells. 2007; 25(1):88–97. [PubMed: 16960136]
34. Müller S, Chakrapani BP, Schwegler H, et al. Neurogenesis in the dentate gyrus depends on ciliary neurotrophic factor and signal transducer and activator of transcription 3 signaling. Stem Cells. 2009; 27(2):431–41. [PubMed: 19023034]
35. Rincón M, Flavell RA, Davis RA. The JNK and P38 MAP kinase signaling pathways in T cell-mediated immune responses. Free Radic Biol Med. 2000; 28:1328–1337. [PubMed: 10924852]
36. Qi M, Elion EA. MAP kinase pathways. J Cell Sci. 2005; 118:3569–3572. [PubMed: 16105880]
37. García-Moreno F, Vasistha NA, Trevia N, et al. Compartmentalization of cerebral cortical germinal zones in a lissencephalic primate and gyrencephalic rodent. Cereb Cortex. 2012; 22(2): 482–92. [PubMed: 22114081]
38. Fujimoto S, Negishi M, Katoh H. RhoG promotes neural progenitor cell proliferation in mouse cerebral cortex. Mol Biol Cell. 2009; 20(23):4941–50. [PubMed: 19812248]
39. Loulier K, Lathia JD, Marthiens V, et al. beta1 integrin maintains integrity of the embryonic neocortical stem cell niche. PLoS Biol. 2009; 7(8):e1000176. [PubMed: 19688041]
40. Lanner F, Rossant J. The role of FGF/Erk signaling in pluripotent cells. Development. 2010; 137:3351–3360. [PubMed: 20876656]
41. Samuels IS, Karlo JC, Faruzzi AN, et al. Deletion of ERK2 mitogen-activated protein kinase identifies its key roles in cortical neurogenesis and cognitive function. J Neurosci. 2008; 28:6983–6995. [PubMed: 18596172]
42. Sato T, Shimazaki T, Naka H, et al. FRS2α regulates Erk levels to control a self-renewal target Hes1 and proliferation of FGF-responsive neural stem/progenitor cells. Stem Cells. 2010; 28:1661–1673. [PubMed: 20652960]
43. Shankaran H, Wiley HS. Oscillatory dynamics of the extracellular signal-regulated kinase pathway. Curr Opin Genet Dev. 2010; 20:650–655. [PubMed: 20810275]
44. Reaume AG, Elliott JL, Hoffman EK, et al. Motor neurons in Cu/Zn superoxide dismutase-deficient mice develop normally but exhibit enhanced cell death after axonal injury. Nat Genet. 1996; 13(1):43–7. [PubMed: 8673102]
45. Carlsson LM, Jonsson J, Edlund T, et al. Mice lacking extracellular superoxide dismutase are more sensitive to hyperoxia. Proc Natl Acad Sci U S A. 1995; 92(14):6264–6268. [PubMed: 7603981]

46. Melov S, Schneider JA, Day BJ, et al. A novel neurological phenotype in mice lacking mitochondrial manganese superoxide dismutase. Nat Genet. 1998; 18(2):159–163. [PubMed: 9462746]

47. Melov S, Coskun PE, Wallace DC. Mouse models of mitochondrial disease, oxidative stress, and senescence. Mutat Res. 1999; 434(3):233–42. [PubMed: 10486594]

48. Noble M, Mayer-Pröschel M, Pröschel C. Redox regulation of precursor cell function: insights and paradoxes. Antioxid Redox Signal. 2005; 7:1456–1467. [PubMed: 16356108]

49. Fang H, Chen M, Ding Y, et al. Imaging superoxide flash and metabolism-coupled mitochondrial permeability transition in living animals. Cell Res. 2011; 21(9):1295–304. [PubMed: 21556035]

50. Ma Q, Fang H, Shang W, et al. Superoxide flashes: early mitochondrial signals for oxidative stress-induced apoptosis. J Biol Chem. 2011; 286(31):27573–27581. [PubMed: 21659534]

51. Wang X, Jian C, Zhang X, et al. Superoxide flashes: elemental events of mitochondrial ROS signaling in the heart. J Mol Cell Cardiol. 2012; 52(5):940–8. [PubMed: 22405973]

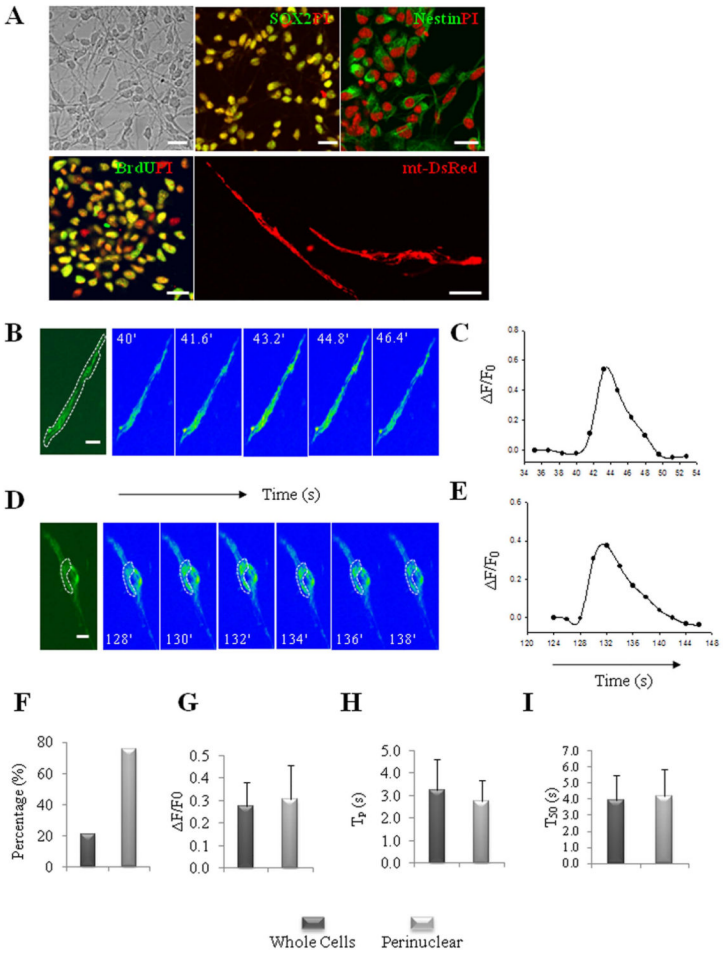

Figure 1.

Characterization of spontaneous mitochondrial SO flashes in NPCs. **(A):** Dissociated NPCs at day 3 in culture were immunostained with antibodies against Sox2, nestin and BrdU (after a 16 h exposure to 10 μM BrdU) (green), which are markers of proliferating NPCs. The nuclei of NPCs were counterstained with propidium iodide (red). The image at the lower right shows NPCs transfected with an mt-DsRed plasmid to illustrate the mitochondrial morphology in NPCs. Bar = 20 μm. **(B-E):** Characteristics of mitochondrial SO flashes in NPCs. Time-lapse images of SO flashes in NPCs **(B, D)** and results of quantification of mt-cpYFP fluorescence intensity before, during and after a SO flash **(C, E)**; the bipolar NPC in panel B exhibited a flash that occurred in all mitochondria throughout the cell, and the rounded cell in panel D exhibited a flash only in perinuclear mitochondria. Bar = 5 μm. **(F):** Percentages of NPCs exhibiting whole-cell and perinuclear flashes. **(G-I):** Distribution and kinetics of whole-cell and perinuclear SO flashes in NPCs. $\Delta F/F_0$ is the amplitude of SO flashes where F_0 refers to basal fluorescence intensity **(G)**; T_p is the time to peak fluorescence intensity **(H)**; and T_{50} is 50% decay time after the peak **(I)**. Values are the mean ± SD (n = 17–63 SO flashes analyzed).

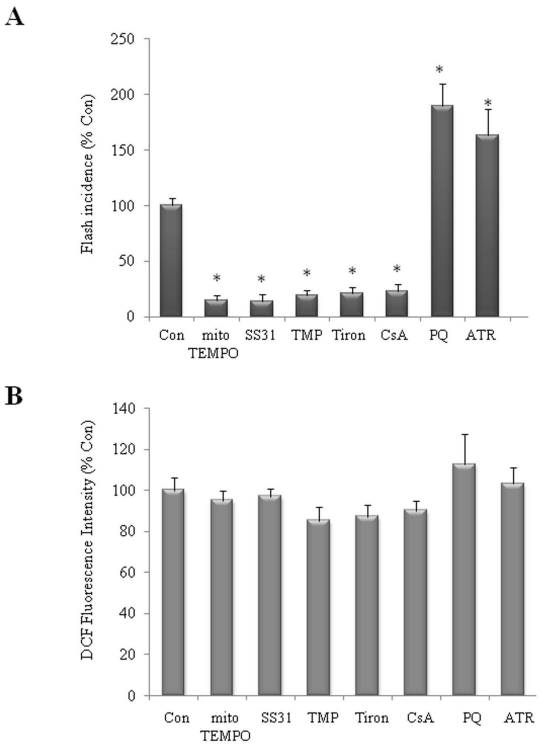

Figure 2.

Mitochondrial SO flash activities are modified by SO scavengers/donors and mPTP inhibitor/opener and doesn′t contribute appreciably to global ROS. **(A):** Mitochondrial SO flashes are suppressed by treatment of NPCs with mitochondrial SO scavengers (MitoTEMPO 1μM and SS31 50μM), the SO mimetic agent (TMP 1 μM), a SO scavenger (Tiron 100 μM) and an inhibitor of mPTP (CsA 0.1 μM). Mitochondrial SO flashes are enhanced by treatment of SO generator (PQ1 μM), mPTP opener (ATR 1 μM). NPCs were treated for 24 h (n = 3 separate experiments; ~100 cells imaged in each experiment). *p<0.05. **(B):** Global ROS levels in NPCs measured by DCF loading were not altered by different treatment as indicated that either suppressed or enhanced SO flash activity. Values are the mean ± SD (n = 3 separate experiments). *p<0.05.

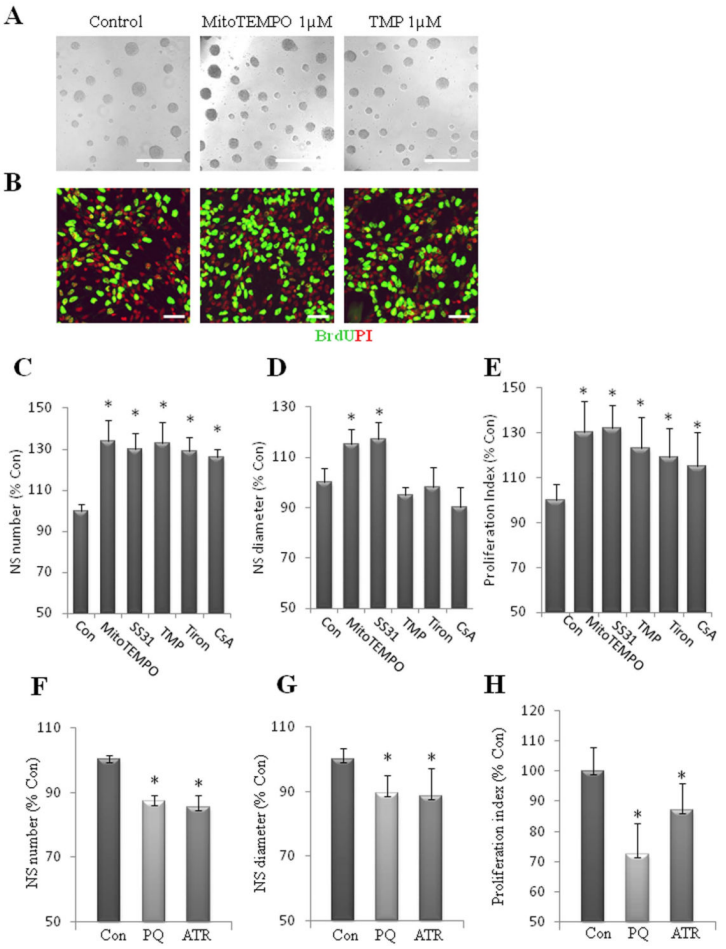

Figure 3.

Superoxide flashes negatively regulate NPC proliferation. **(A):** Images of neurospheres in cultures which had been treated for 6 d with vehicle (Control) or 1 μM MitoTEMPO, 1 μM TMP. Bar = 500 μm. **(B):** Images of dissociated adherent NPCs in cultures which had been treated as indicated in **(A)**. The NPC were then incubated for 2 h in the presence of BrdU (10 μM), fixed and immunostained with antibodies against BrdU (green) and propidium iodide (PI; red). Bar = 40 μm. **(C, D):** Results of quantification of neurosphere number **(C)** and diameter **(D)** in cultures maintained for 6 d in the presence of MitoTEMPO 1μM, SS31 50μM, TMP 1 μM, Tiron 100 μM and CsA 0.1 μM. **(E):** Quantitative analysis of proliferation index ($BrdU^+$ cells/total cells) in dissociated NPC cultures treated for 24 h with the indicated treatments in **(C)** and **(D)**. **(F, G):** Results of quantification of neurosphere number **(F)** and diameter size **(G)** in cultures maintained for 6 d in the presence of 1 μM PQ or 1 μM ATR. **(H):** Quantitative analysis of proliferation index (BrdU+ cells/total cells) in dissociated NPC cultures treated for 24 h with the indicated treatments. Values are expressed as a percentage of the mean of the control condition (n = 3 separate experiments) *$p<0.05$.

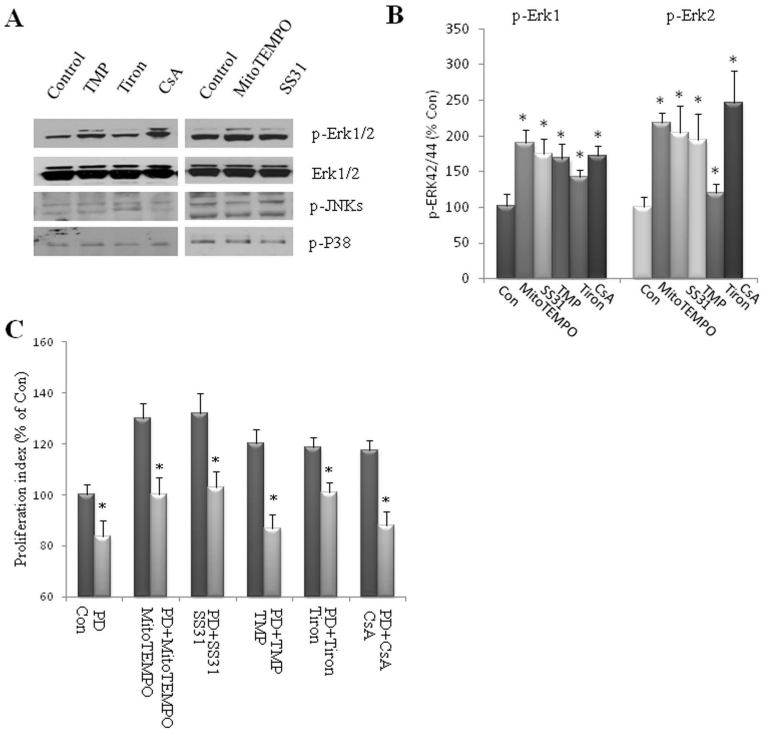

Figure 4.

Suppression of superoxide flash promotes ERK1/2 phosphorylation. **(A, B):** Dissociated adherent NPCs were treated with 1μM MitoTEMPO, 50μM SS31, 1 μM TMP, 100 μM Tiron or 0.1 μM CsA for 24 h. Immunoblot analysis using antibodies that selectively recognize phosphorylated (active) forms of ERKs 1 and 2, p38 or JNK. Blots were reprobed with phosphorylation-insensitive antibodies against ERKs 1 and 2. Panel A show representative blots and panels B show results of densitometric analysis of 4-6 blots. *p<0.05 compared to the control value. **(C):** Quantitative analysis of proliferation index (BrdU+ cells/total cells) in dissociated NPC cultures which were pretreated for 1 h with PD98059 20 μM, and were then treated for 24 h with vehicle (con), 1μM MitoTEMPO, 50 μM SS31, 1 μM TMP, 100 μM Tiron or 0.1 μM CsA. *p<0.05 compared to the corresponding value for cultures treated without PD98059.

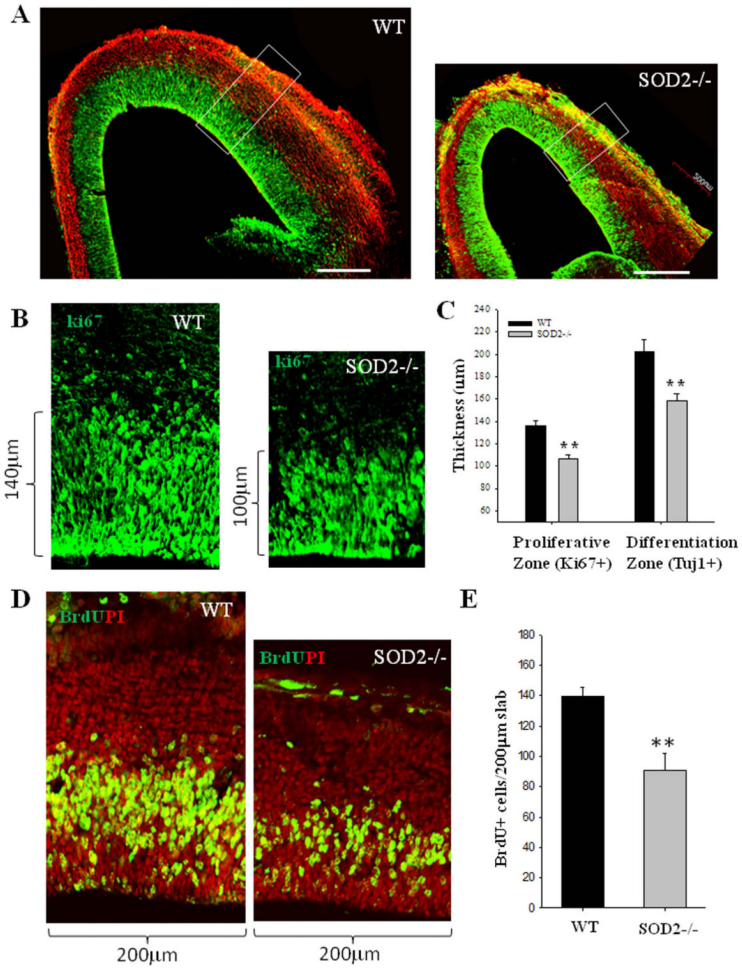

Figure 5. SOD2 deficiency results in a significant reduction in the size of the proliferative zone and NPC proliferation in the embryonic cerebral cortex

(A): Representative confocal images showing Ki67 (green) and Tuj1 (red) immunoreactive cells in brain sections from E14.5 wild type and SOD2−/− littermate embryos, taken from matched sections at the same level of the frontal cortex. **(B)**: representative higher-magnification confocal images of a 200 μm slab of the middle telencephalon wall as indicated in (A) are shown with Ki67 (green) staining. **(C)**: The combination of Ki67 (proliferation marker) and Tuj1 (a marker of differentiated neurons) delineates the zones of cell proliferation and differentiation (A). The thicknesses of proliferative zone (Ki67+) and differentiation zone (Tuj1+) were quantified and values represent the mean ± SD of analyses performed on brain sections from 3 WT and 3 SOD2−/− mice. *p<0.05 and **p<0.001. **(D)**: Representative confocal images of a 200 μm slab of the middle telecencephalon wall of WT and SOD2−/− littermate mice at E14.5 immunostained with BrdU (green) and propidium iodide (PI; red). Pregnant dams at E14.5 were pulse (1h) labeled with BrdU, and brain sections were immunostained with BrdU (green) and counterstained with PI (red). **(E):** Total BrdU+ cells within a 200 μm slab of the middle telecencephalon wall of WT and SOD2−/− littermate mice were quantified. Values represent the mean ± SD of analyses performed on brain sections from 3 WT and 3 SOD2−/− mice. **p<0.01.

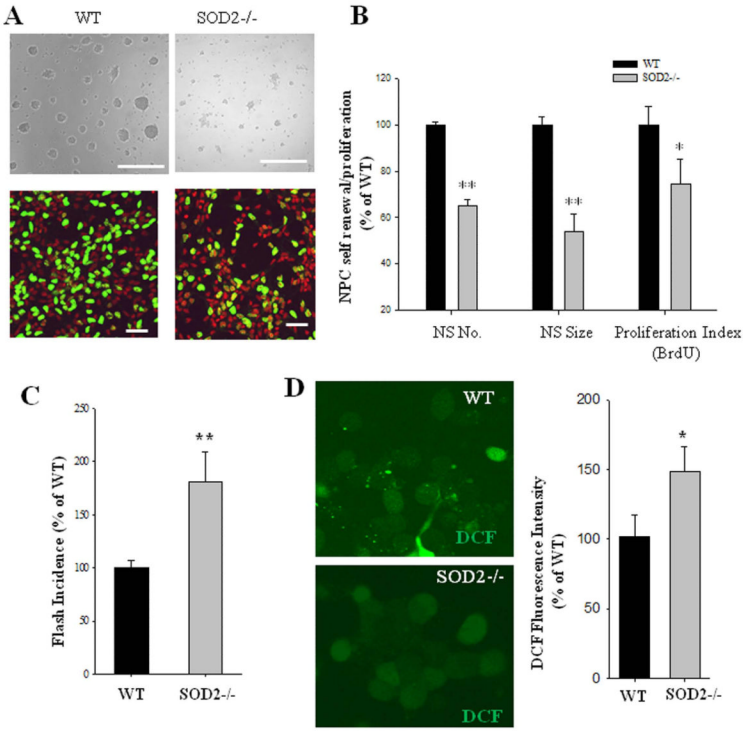

Figure 6. NPCs lacking SOD2−/− exhibit increased mitochondrial SO flash incidence and a reduction of cell proliferation

(A): Representative images of neurospheres in cultures prepared from E14.5 cerebral cortex of WT and SOD2−/− littermate mice, and representative images of dissociated adherent NPCs in cultures which were incubated for 2 h in the presence of BrdU (10 μM), fixed and immunostained with antibodies against BrdU (green) and PI (red). Bar = 40 μm. **(B):** Results of quantification of neurosphere number, diameter size and proliferation index (BrdU+ cells/total cells) in dissociated NPC cultures established from WT and SOD2−/− mice. Values are expressed as a percentage of the mean of the control condition (n = 8 pairs of WT and SOD2−/− NPC cultures. *p<0.05 and **p<0.01. **(C)**: mitochondrial superoxide flashes are enhanced in SOD2−/− NPC in comparison to that of WT. NPCs were imaged on culture day 3 (n = 3 pairs of littermate NPC cultures; ~100 cells imaged in each experiment). **p<0.01. **(D):** Global ROS levels in NPCs measured by DCF loading were also increased. Representative images of DCF fluorescence in WT and SOD2−/− NPC are shown, and the quantitative data of DCF fluorescence intensity are expressed as the percentage of the WT control levels. Values are the mean ± SD (n = 3 separate experiments). ** p<0.01.

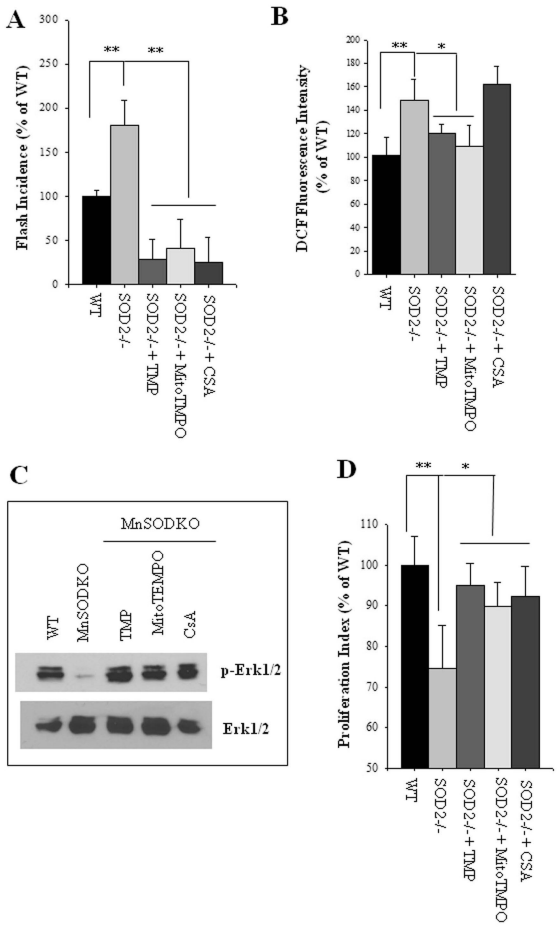

Figure 7. Mitochondrial mPTP-dependent bursts of SO production mediate impaired proliferation of NPC caused by SOD2−/− deficiency

(A): Dissociated adherent NPCs from SOD2−/− mice were treated for 6 h with 1μM TMP, 1μM MitoTEMPO, or 0.1μM CsA. Results show analysis of SO flash incidence (number of NPCs which exhibited a mitochondrial SO flash among ~150 cells imaged for 3 minutes). **(B):** Global ROS levels in NPCs measured using the probe DCF. **(C):** Immunoblot of p-ERK1/2 and total ERK1/2 in cortical NPCs from wild type mice (WT) or Mn-SOD deficient mice (MnSODKO) that had been treated for 6 h with 1 μM TMP, 1μM MitoTEMPO or 0.1μM CsA. p-ERK1/2 levels were reduced in NPCs lacking SOD2 and treatment with TMP, MitoTEMPO and CsA restored p-ERK levels. **(D)**: Results of quantification of proliferation index (BrdU+ cells/total cells) in dissociated NPC cultures from WT and SOD2−/− mice. NPCs were treated for 24 h with 1 μM TMP, 1μM MitoTEMPO, 0.1μM CsA, or vehicle control. All data in A-C are plotted as the percentage of WT control. *p<0.05 and **p<0.01 WT compared to SOD2−/−, or treatment compared to vehicle control.